THE JOURNAL OF PHYSICAL CHEMISTRY C

Article

Cite This: J. Phys. Chem. C 2019, 123, 8265−8272

pubs.acs.org/JPCC

Carboxylic Anchoring Dye *p*-Ethyl Red Does Not Adsorb Directly onto TiO_2 Particles in Protic Solvents

Hui Fang,[†] Jianqiang Ma,[†] Michael J. Wilhelm,[†] Yi Rao,[†,§] Danielle L. Kuhn,[‡] Zachary Zander,[‡] Brendan G. DeLacy,[‡] and Hai-Lung Dai*[,†]

[†]Department of Chemistry, Temple University, Philadelphia, Pennsylvania 19122, United States

[‡]U.S. Army Edgewood Chemical Biological Center, Research & Technology Directorate, Aberdeen Proving Ground, Maryland 21010, United States

ABSTRACT: Adsorption of the carboxylic anchoring dye, *p*-ethyl red (*p*-ER), onto TiO_2 nanoparticles in protic vs aprotic solvents was studied *in situ* using the surface-specific technique, second harmonic light scattering (SHS). Two different adsorption schemes were proposed to account for *p*-ER interactions with TiO_2 under different solvent environments. In aprotic solvents, *p*-ER adsorbs directly onto TiO_2. Conversely, in protic solvents, in which solvent molecules bind stronger than *p*-ER with TiO_2, the dye molecules adsorb onto the solvent shell around the particle but not directly to the TiO_2 surface. In addition, a portion of the *p*-ER molecules form hydrogen bonds with the protic solvent molecules. The two different adsorption models reproduce the measured adsorption isotherms detected by SHS. Specifically, the *p*-ER molecules adsorb with a smaller free energy change and a larger density in protic solvents than in aprotic solvents. Our results indicate that protic solvents are undesirable for administering adsorption of carboxylic dyes in dye-sensitized solar cell applications as the dye molecules do not directly adsorb onto the TiO_2 particle.

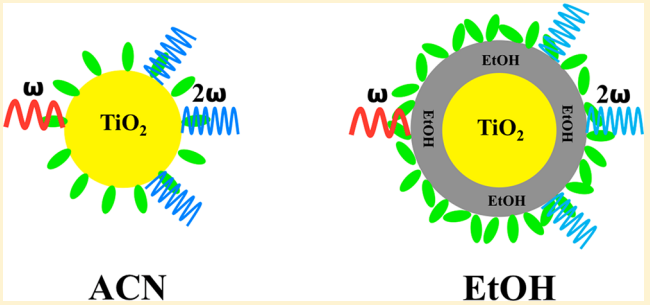

I. INTRODUCTION

Dye-sensitized solar cells (DSSC), a third-generation solar cell technology, have been in development since O'Regan and Gratzel's 1991 report.[1] In DSSC, excited carriers are first generated in light-absorbing organic dyes adsorbed on a semiconductor surface and are subsequently transported into the semiconductor particles.[1,2] TiO_2 is a well-known semiconductor for DSSC because of its desirable bandgap as well as the fact that it is nontoxic and easy-to fabricate.[3−5] The selection of the dye is based on its ability to absorb light, its energetics relative to the semiconductor bands, and its interaction with the semiconductor surface to facilitate charge transfer.[6,7] Dye molecules containing carboxylic groups are routinely employed due to these considerations.[1,8,9] The overall efficiency of a DSSC depends on the number of dye molecules adsorbed at the semiconductor surface and the electron injection rate from the dye to the semiconductor,[10,11] both of which depend on interactions between the dye and the semiconductor[12−14] and are known to be affected by the solvents used in the dye adsorption process.[15−18]

In general, solvents can be classified into two categories based on their ability to donate protons, protic and aprotic.[19] Protic solvents, such as ethanol and 2-propanol, can donate protons easily and enable hydrogen bonding among neighboring solvent molecules and between dye and solvent molecules. In contrast, for aprotic solvents (such as acetonitrile), the interactions are typically through dispersion forces. We have previously characterized the effect of several aprotic solvents on the adsorption of the dye, *p*-ethyl red (*p*-ER), at the TiO_2 particle surface.[13] It was found that more polar solvents (e.g., acetonitrile) resulted in larger adsorption free energies. Additionally, an ultrafast transient absorption study of electron injection from *p*-ER to the TiO_2 surface showed faster injection rates as solvent polarity increases.[20] These results demonstrated that polar aprotic solvents are a better choice for DSSC fabrication with dyes containing carboxyl anchoring groups.

We note that protic solvents have also been tested in the DSSC fabrication process.[18,21] For example, for Monascus Red dye-sensitized solar cells, protic solvents such as water and ethanol were found to give lower conversion efficiency than the polar aprotic solvent, dimethyl sulfoxide (DMSO).[21] In another study, it was found that adsorption number density of an infrared organic dye (NK-6037) on TiO_2 increased dramatically in alcoholic solvents with decreasing dielectric constants.[18] However, the general understanding of how protic solvents affect dye adsorption on TiO_2 is still lacking.

Special Issue: Hans-Joachim Freund and Joachim Sauer Festschrift

Received: August 31, 2018
Revised: January 26, 2019
Published: February 6, 2019

DOI: 10.1021/acs.jpcc.8b08513
J. Phys. Chem. C 2019, 123, 8265−8272

It is anticipated that dyes with carboxylic groups will be subjected to hydrogen bonding in protic solvents, in contrast to the absence of hydrogen bonding in aprotic solvents. Hydrogen bonding to solvent molecules should reduce the tendency for the dye to bind to the TiO_2 surface. Furthermore, alcoholic protic solvent molecules may form strong covalent bonds with the semiconductor surface,[22−25] which would subsequently hinder interactions between the carboxylic dyes and TiO_2.

To quantitatively determine the adsorption characteristics for dyes interacting with TiO_2 colloidal particles we use the surface specific technique, second harmonic light scattering (SHS).[26−34] SHS signal can be generated from molecules aligned on the surface of a particle. SHS has been demonstrated as a versatile tool for accurate measurement of the adsorption density and free energy of molecules on colloidal particle surfaces and has already be applied to characterize adsorption of a carboxyl anchoring dye onto TiO_2 particle surfaces in aprotic solvents.[13]

In this study, ethanol and 2-propanol were chosen as representative protic solvents in which adsorption of *p*-ER onto the surface of TiO_2 nanoparticles was measured by SHS. The adsorption characteristics are compared with those measured for the aprotic solvent acetonitrile. It is found that strong binding of protic solvent molecules prohibits direct adsorption of *p*-ER directly onto the TiO_2 particle surface.

II. MATERIALS AND METHODS

Materials. Titanium oxide nanopowder/nanoparticles (TiO_2, rutile, high purity, 99.9%, 165 nm) was obtained from US Research Nanomaterials Inc. The average size was characterized by scanning electron microscopy (SEM) to be 160 ± 40 nm in diameter. Rutile (110) has the dominating presence at the TiO_2 particle surface based on powder X-ray diffraction measurements.[13] Additional characteristics of the TiO_2 particle can also be found on the company's Web site. Acetonitrile (ACN, ≥99.93%) and 2-propanol (IPA, ≥99.5%)) were purchased from Sigma-Aldrich. Ethanol (EtOH, 200 proof-Absolute, Anhydrous) was purchased from Pharmco-Aaper Inc. *p*-Ethyl Red (*p*-ER) dye was synthesized according to the procedure reported in our previous publication.[13] A typical particle density of roughly 3.9×10^9 TiO_2 particles/mL was used for the SHS experiments.

Second Harmonic Light Scattering (SHS). The experimental setup used in this work has been previously described.[13] Briefly, the output of a Ti:sapphire oscillator (Coherent Micra-5, average power 350 mW, 80 MHz repetition rate, 50 fs pulse duration) at 800 nm was used as the fundamental for the SHS measurement. The laser beam was focused at the center of a glass tube (inner diameter 0.8 cm, outer diameter 1.0 cm) containing the colloidal suspension of TiO_2 particles. A magnetic stirrer was placed inside the tube to ensure homogeneous mixing of the dye and TiO_2 particles. A photomultiplier tube (R1527, Hamamatsu) operated at 1000 V and interfaced with a single photon counting system (Stanford Research System SR400) was used to detect the SHS signal. A long pass filter was placed before the sample to remove any second harmonic (SH) signal from materials in the path of the fundamental beam, and a short pass filter was used to filter out the fundamental light before the monochromator (Acton 300, Grating 300 grooves/mm, blazed at 500 nm). All experiments were performed at room temperature (22 ± 1 °C). The stir bar and glass tubes were cleaned with piranha solution (H_2O_2:H_2SO_4 volume ratio 3:7), rinsed thoroughly with deionized water (18.2 MΩ·m), and then dried before experiments.

Dynamic Light Scattering (DLS). The hydrodynamic size of TiO_2 nanoparticles (NPs) in different solvents were measured with a Malvern Zetasizer Nano ZSP. Similar to the SHS experiments, a density of 3.9×10^9 TiO_2 particles per mL solution was used for the DLS measurements. The dielectric constants[35,36] used for ACN, EtOH, and IPA are 37.5, 24.3, 18.3, respectively. The refractive index[35] used for ACN, EtOH, and IPA are 1.342, 1.359, and 1.383, respectively. Measurements were conducted at (25.0 ± 0.1) °C with the 632.8 nm laser output. A total of three measurements were acquired for each sample.

Fourier Transform Infrared (FTIR) Spectroscopy. FTIR spectra were recorded on a Thermo Nicolet Magna 860 FTIR spectrometer with a spectral resolution of 0.5 cm^{-1} averaging 128 scans, equipped with a MCT detector cooled by liquid nitrogen. A homemade sample holder assembly, which has an optical path-length of a 25 μm (defined by a plastic spacer), was used to allow measurements of the solute in solvent and solvent spectra in a single experiment. The final reported results correspond to the absorbance of the solute, in which the pure solvent signal has been removed by subtraction.

Computational Methods. *Ab initio* calculations were performed in order to deduce the magnitude and spatial orientation of the frequency-dependent first hyperpolarizability tensor elements, $\beta(-2\omega;\omega,\omega)$, for *p*-ER under different solvent conditions. Specifically, time-dependent density functional theory (TD-DFT), using the Coulomb attenuating method (CAM),[37] was used to characterize the 10 lowest energy excited electronic states of *p*-ER at the cam-B3LYP/6-311+G(2d,p) level of theory. Frequency dependent hyperpolarizabilities were calculated using the *Polar CPHF = (RdFreq)* keyword. Solvent effects were modeled using the *SCRF = (PMC, Solvent = ***)* keyword in which the solvent was specified as either ethanol or acetonitrile. Additionally, TD-DFT was used to deduce the magnitude and spatial orientation of the electronic transition dipole moments for transitions from the ground state to the ten lowest energy electronic states. All calculations were performed in the GAUSSIAN09 suite of programs.[38]

III. RESULTS

Particle Size in Different Solvents. Solvent molecules may bind to TiO_2 particles with different strength. Molecules bound to particles through covalent bonds would appear in dynamic light scattering (DLS), which measures the hydrodynamic size of the particle moving in the solvent, together with the solvent shell as part of the particle. DLS measurements of TiO_2 particles in ACN (red line), EtOH (black line), and IPA (blue line) are shown in Figure 1. The experimental data was fit to a Gaussian function to deduce the average hydrodynamic size distribution of TiO_2, which was found to be 310 ± 73, 483 ± 134, and 444 ± 156 nm for ACN, EtOH, and IPA, respectively. It is noted that the hydrodynamic size (diameter) of TiO_2 colloids in the protic solvents, EtOH and IPA, are 100 nm larger than in the aprotic ACN. This increased size indicates that the protic solvent molecules bond strongly with the TiO_2 particle and therefore form a molecular solvent shell around the particle. In the absence of solvents, SEM measurements reveal that the average size of TiO_2 nanoparticles is 160 ± 40 nm, which is roughly 150, 320,

DOI: 10.1021/acs.jpcc.8b08513
J. Phys. Chem. C 2019, 123, 8265−8272

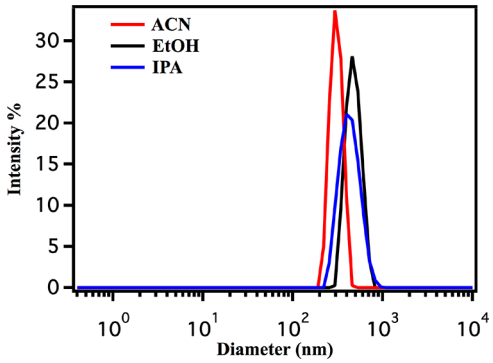

Figure 1. Dynamic light scattering measurement of TiO_2 particles in ACN (red line), EtOH (black line), and IPA (blue line). The average hydrodynamic size distribution in ACN, EtOH, and IPA is 310 ± 73, 483 ± 134, and 444 ± 156 nm, respectively.

and 280 nm smaller than the hydrodynamic size in ACN, EtOH, and IPA, respectively. The substantially thicker solvation shells observed for EtOH and IPA (>150 nm) likely stems from stronger bonding of the solvent with TiO_2.

Second Harmonic Light Scattering. It has been shown that *p*-ER can facilitate second harmonic generation (SHG) following irradiation with 800 nm light. The resulting 400 nm SH light is resonantly enhanced.[13] As *p*-ER adsorbs onto a surface, molecule−surface interactions (as well as interadsorbate interactions) align the adsorbed *p*-ER molecules so that the SH light generated by these molecules constructively interfere. Conversely, SH light generated by randomly oriented *p*-ER molecules in solution destructively interfere and cancel with each other. Consequently, SHS signal detected from samples containing colloidal TiO_2 and *p*-ER reflects the amount of *p*-ER adsorbed on the particle surface.

Figure 2 displays the SHS intensities measured as a function of the *p*-ER concentration added into the TiO_2 colloid in

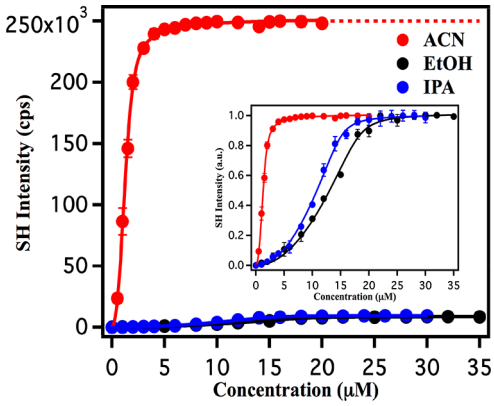

Figure 2. Experimentally measured adsorption isotherm of *p*-ER onto TiO_2 nanoparticle surface in ACN (red dots), EtOH (black dots), and IPA (blue dots). The solid curves are fits based on different Langmuir adsorption models: eq 3 for ACN and eq 6 for EtOH and IPA. Inset shows the normalized SH intensity curves.

different solvents. The SHS intensity at each data point was recorded after it reached a constant value following the addition of the dye, indicating that equilibrium has been reached at that specific *p*-ER concentration. The red dots are the SH intensities from *p*-ER molecules adsorbed on TiO_2 in ACN. The SH signal reached saturation at the low concentration of only ca. 5 μM. The black dots are SH intensities from *p*-ER adsorbed on TiO_2 in EtOH, where the signal reaches saturation at ca. 25 μM. Blue dots are from *p*-ER adsorbed on TiO_2 in IPA, where saturation is observed at ca. 20 μM, similar to the EtOH result. The maximum SH intensity of *p*-ER adsorbed on the TiO_2 surface in ACN is almost 25 times larger than the signal for either EtOH or IPA. The insert in Figure 2 shows the SH intensity as a function of *p*-ER concentration with the maximum of each SHS curve normalized to the same magnitude.

Next, we consider competing solvent effects on the adsorption of *p*-ER on the TiO_2 surface. Specifically, we monitor changes in the measured SH intensity from a sample containing colloidal TiO_2 in ACN, a constant concentration of *p*-ER, and increasing concentrations of EtOH. Figure 3 shows

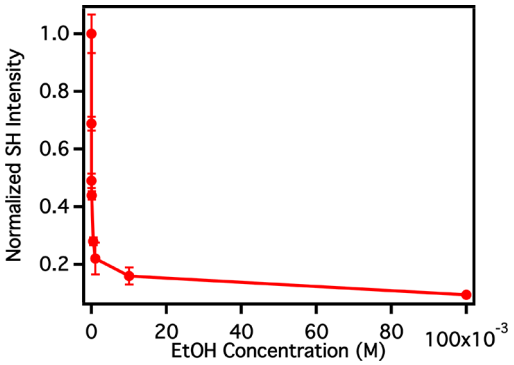

Figure 3. Normalized SHS signal from a sample containing 10 μM *p*-ER and TiO_2 in ACN colloid as a function of EtOH concentration added. The decrease of the SHS signal indicates that EtOH can displace adsorbed *p*-ER molecules from the TiO_2 surface in ACN.

the normalized SHS signal from 10 μM *p*-ER interacting with TiO_2 in ACN colloid, as a function of EtOH concentration added. The first point is the measured SH signal without EtOH and was normalized to 1. Importantly, the SHS signal is observed to decrease as the concentration of EtOH increases. Specifically, the SHS signal decreases to 0.5 when 10 μM EtOH was added (i.e., corresponding to equal parts *p*-ER and EtOH) and the signal decays to less than 0.1 when 0.1 M EtOH was added.

IV. ANALYSIS

The SHS intensity, I_{SHS}, can be quantitatively analyzed for extraction of information such as the adsorption free energy and the density of surface adsorbed dye. Experimentally, I_{SHS} is related to the square of the *p*-ER surface coverage, θ, which is defined as the ratio of the number of surface adsorbed dye molecules (N) to the maximum number of adsorption sites (N_{max}) on the nanoparticle surface:[26,39−41]

$$I_{SHS} \propto A\theta^2 \quad (1)$$

Here A is a proportionality scaling constant that is intrinsically related to the ensemble average of the hyperpolarizability of *p*-ER adsorbed on the particle surface.

***p*-ER in Aprotic Solvents.** The surface coverage of *p*-ER on the TiO_2 surface at any given dye concentration in the colloidal solution can be quantitatively described by the Langmuir model. For an aprotic solvent like ACN the coverage is determined by the adsorption equilibrium:

DOI: 10.1021/acs.jpcc.8b08513
J. Phys. Chem. C 2019, 123, 8265−8272

Table 1. Fitting Parameters, Including the Proportionality A Constant and the Maximum Number N_{max} of p-ER Adsorbed onto TiO_2 Particles, the Binding Constant K in ACN, and the Scaled αK in EtOH and IPA[a]

aprotic	ACN	protic	EtOH	IPA
A	257800 ± 998	A	8672 ± 148	9478 ± 133
N_{max} (μM)	1.58 ± 0.04	N_{max} (μM)	18.2 ± 0.4	15.0 ± 0.3
$19/K$ (μM)	0.08 ± 0.01	$1/\alpha K$ (μM)	0.13 ± 0.06	0.11 ± 0.04
K	$(2.4 \pm 0.3) \times 10^8$	αK (M^{-1})	$(7.5 \pm 3.4) \times 10^6$	$(8.8 \pm 3.4) \times 10^6$
ΔG (kcal/mol)	−11.4 ± 0.1	ΔG (kcal/mol)	−9.4 ± 0.2	−9.5 ± 0.2

[a]The free energy ΔG is calculated from K or αK.

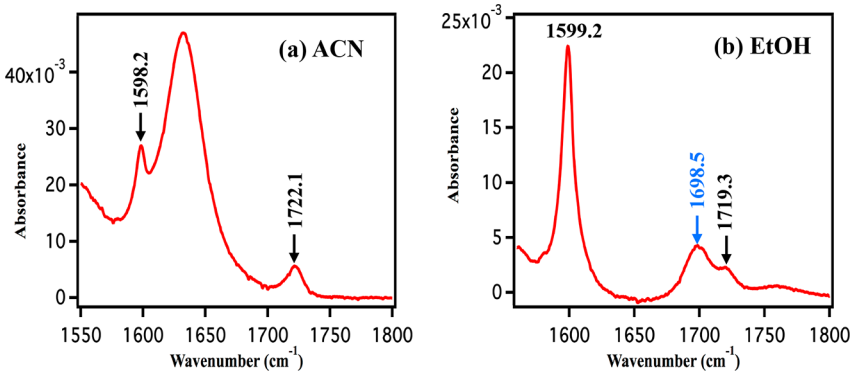

Figure 4. FTIR spectra of p-ER in ACN (a) and EtOH (b). Peaks at 1598.2 and 1599.2 cm^{-1} correspond to aromatic modes. Peaks at 1722.1 and 1719.3 cm^{-1} correspond to COOH stretches. The new peak at 1698.5 cm^{-1} (in EtOH) is the hydrogen-bonded COOH stretch. The broad band near 1640 cm^{-1} in the ACN spectrum corresponds to residual signal from the ACN solvent not removed from the subtraction procedure.

$$\mathrm{D} + \mathrm{TS} \underset{k_d}{\overset{k_a}{\rightleftharpoons}} \mathrm{DT} + \mathrm{S} \tag{2}$$

Here a p-ER dye molecule (D) moves onto a surface adsorption site (TS), displaces an adsorbed solvent molecule (S) from the surface into the solution, and becomes adsorbed (DT). The adsorption and desorption rates are denoted as k_a and k_d, respectively. θ is related to the total concentration of p-ER in solution:[27,29,30]

$$\theta = \frac{N}{N_{max}} = \frac{\left(C + N_{max} + \frac{19}{K}\right) - \sqrt{\left(C + N_{max} + \frac{19}{K}\right)^2 - 4CN_{max}}}{2 \cdot N_{max}} \tag{3}$$

where N_{max} and the adsorption equilibrium constant, $K = k_a/k_d$, can be obtained from a nonlinear least-squares fit of the adsorption isotherm in Figure 2. K can then be used to calculate the adsorption free energy ΔG_{ads}. The numerical constant 19 corresponds to the molar concentration of pure ACN in units of mol/L.

The fit deduced N_{max} for p-ER on TiO_2 in ACN is 1.58 ± 0.04 μM (Table 1), which is similar to the theoretical maximum number 1.5 μM. The adsorption free energy is −11.4 ± 0.1 kcal/mol.

***p*-ER in Protic Solvents.** Adsorption of p-ER onto TiO_2 in protic solvents, such as EtOH and IPA, differs from that in aprotic solvents due to two primary considerations: (1) p-ER can form hydrogen bonds with solvent molecules, and (2) protic solvent molecules strongly bind to the TiO_2 surface.

The existence of hydrogen bonded p-ER can be identified in the IR absorption spectrum. Figure 4 depicts the FTIR absorption spectra for p-ER and TiO_2 in ACN (Figure 4a) and EtOH (Figure 4b). All the observed spectral resonances can be assigned as follows except the broad band near 1640 cm^{-1} in the ACN spectrum which is an artifact resulting from the subtraction procedure aimed at removing the signal from the ACN solvent. The bands at 1598.2 and 1599.2 cm^{-1} correspond to the aromatic modes ($\nu_{aromatic}$) of p-ER in ACN and EtOH, respectively. Likewise, the bands at 1722.1 and 1719.3 cm^{-1} are the C═O stretch mode (ν_{COOH}) of the carboxylic groups of p-ER in ACN and EtOH, respectively. The peak at 1698.5 cm^{-1} in EtOH, but not in ACN, is assignable to hydrogen bonded carboxylic groups of p-ER. The measured intensity ratio between hydrogen bond COOH (1698.5 cm^{-1}) and free COOH (1719.3 cm^{-1}) is roughly 2:1, strongly suggesting that the ratio of hydrogen bonded COOH to free COOH is about 2:1.

Protic solvents like EtOH and IPA bind strongly to TiO_2.[22,42] The strong binding is supported by the particle size measurements described in the previous section. Furthermore, previous studies have reported that the adsorption free energy for a hydroxyl group (−OH) interacting with a TiO_2 surface is comparable to that of a carboxyl group (−COOH).[24,43−45] We therefore expect that, in alcoholic solvents, it is unlikely that p-ER will displace a solvent molecule from the TiO_2 surface. This is especially true for our experimental conditions in which the p-ER concentration is orders of magnitude smaller than the solvent (i.e., μM vs M). Instead, we anticipate that p-ER would predominantly adsorb onto the solvent shell around the TiO_2 particle.

The adsorption of p-ER can therefore be described by two distinct equilibria: (1) the hydrogen bonding equilibrium for p-ER and solvent molecules forming hydrogen bonded p-ER (represented by DHS)

$$\mathrm{D} + \mathrm{S} \underset{k_{-1}}{\overset{k_1}{\rightleftharpoons}} \mathrm{DHS} \tag{4}$$

DOI: 10.1021/acs.jpcc.8b08513
J. Phys. Chem. C 2019, 123, 8265−8272

Scheme 1. Different Adsorption Models for *p*-ER onto TiO_2 Nanoparticle Surfaces in ACN and EtOH[a]

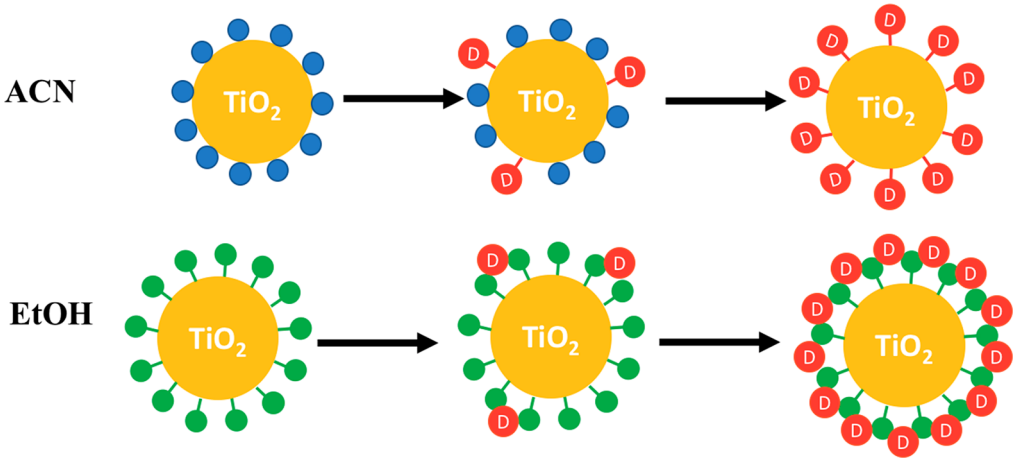

[a]In ACN, *p*-ER can replace the adsorbed ACN and chemically bind with TiO_2. In EtOH, *p*-ER interacts with the EtOH solvation shell covering the TiO_2 particle.

and (2) the adsorption equilibrium of *p*-ER onto a surface site of the solvent shell (represented by DTS)

$$\mathrm{D} + \mathrm{TS} \underset{k_d}{\overset{k_a}{\rightleftharpoons}} \mathrm{DTS} \tag{5}$$

Consequently, the dye surface coverage for protic solvents can be expressed as[46]

$$\theta = \frac{N}{N_{max}} = \frac{\left(C + N_{max} + \frac{1}{\alpha \cdot K}\right) - \sqrt{\left(C + N_{max} + \frac{1}{\alpha \cdot K}\right)^2 - 4CN_{max}}}{2N_{max}} \tag{6}$$

where $\alpha = 1/(17K_1 + 1)$, in which K_1 is the equilibrium constant of eq 4 and K is the equilibrium constant of eq 5. Nonlinear least-squares fittings of SH intensities as a function of *p*-ER concentration in EtOH and IPA yield values of αK and N_{max}.

The N_{max} of *p*-ER on TiO_2 in EtOH and IPA obtained from the fitting (reported in Table 1) are 18.2 ± 0.4 μM and 15.0 ± 0.3 μM, respectively. These are more than 10 times higher than the theoretical maximum number 1.5 μM. The hydrogen bond scaled adsorption free energy of *p*-ER on TiO_2 in EtOH and IPA are −9.4 ± 0.2 and −9.5 ± 0.2 kcal/mol, respectively. Both are 2 kcal/mol less than the adsorption free energy in ACN.

V. DISCUSSION

V.A. Adsorption of *p*-ER on TiO_2 in Protic vs Aprotic Solvents. In our previous report,[13] effects of aprotic solvents on the adsorption of *p*-ER onto TiO_2 nanoparticle surfaces were examined using SHS. We found that more polar solvents, like acetonitrile, result in a larger adsorption free energy change for *p*-ER adsorption. Here, using the same experimental approach, we characterize the effect of protic solvents on the adsorption of *p*-ER on TiO_2 particles. In protic solvents, the solvent molecules bind strongly to the TiO_2 surface and compete against direct dye adsorption onto the particle surface. Further, hydrogen bonding between solvent molecules and *p*-ER reduces the quantity of *p*-ER molecules that may adsorb onto the particle surface.

Hydrogen bonding between the solvent hydroxyl group and the carboxylic group of the dye has already been discussed.[15] Here, hydrogen bonding specifically between EtOH and *p*-ER was confirmed by FTIR measurements (Figure 4).

The interaction of alcohols on TiO_2 surfaces has previously been studied.[42,43] The chemisorption and dissociation of alcohols on TiO_2 surfaces have been observed.[22] Our DLS measurements in Figure 1 show that the TiO_2 hydrodynamic size is 1.5 times bigger in EtOH and IPA when compared with that in ACN: indicating that EtOH and IPA strongly bind onto the TiO_2 particle and form a solvent shell. Consequently, in the presence of protic solvents, *p*-ER likely adsorbs to the solvation shell, rather than the TiO_2 particle surface.

Our analysis shows that the adsorption free energy change for *p*-ER adsorption onto TiO_2 in ACN is roughly 2 kcal/mol larger than in EtOH and IPA. This difference is likely due to the differences in binding sites: i.e., in ACN, *p*-ER adsorbs directly onto TiO_2, whereas in protic solvents, *p*-ER adsorbs onto the solvent shell surrounding the particle. The binding energy between the carboxylic group of *p*-ER with TiO_2 is expected to be stronger than that between the carboxylic group with the solvent molecules surrounding the TiO_2 particle.

The N_{max} for *p*-ER on the particle surface in protic solvents is deduced to be an order of magnitude larger than in the aprotic solvent ACN. We note that N_{max} is the total number of *p*-ER molecules on the surface and is a product of the surface area and the adsorption density.

The unit cell dimension of the Rutile TiO_2 (110) surface is around 6 Å.[47] The carboxylic group binding site on the TiO_2 (110) surface is expected to be 36 $Å^2$, which is consistent with the results suggesting only 1−2 binding sites per nm^2 are available on Anatase p-25 TiO_2.[48] For 160 nm diameter TiO_2 particles, the maximum number of adsorbed molecules (N_{max}) is calculated to be around 1.5 μM. This number compares well with the 1.58 ± 0.04 μM measured for *p*-ER on TiO_2 in ACN. This number is, however, an order of magnitude smaller than the 18 μM and 15 μM values deduced for *p*-ER on TiO_2 particles in EtOH and IPA, respectively.

To rationalize the much larger N_{max} in protic solvents, we first consider that the particle size measured in EtOH and IPA

DOI: 10.1021/acs.jpcc.8b08513
J. Phys. Chem. C 2019, 123, 8265−8272

was 1.5 times larger than in ACN. Correspondingly, the surface area of the particles in the protic solvents is ~2.25 times larger than in ACN. Furthermore, the larger particle sizes in the protic solvents are consistent with the conjecture that there is a solvent shell around the TiO_2 particle and that *p*-ER adsorbs onto the solvent shell. As reflected by the free energy changes measured for the different adsorptions in the two different types of solvents, the dye−protic molecule interaction is weaker than the dye−TiO_2 binding. The weaker interaction depicts that the adsorption of dye on the solvent shell is less site-specific than on the TiO_2 surface. Consequently, the adsorption density on the solvent shell can be larger than on the TiO_2 surface. An estimate based on the measured N_{max} and particle size put the average adsorption site on the particle in the protic solvents as ~2.5 Å^2, a small but not unreasonable number considering that the carboxylic group has a 2−3 Å^2 size.[49]

As shown in Scheme 1, two different solvent-dependent adsorption models are described for interactions of *p*-ER with TiO_2 particles. In ACN, the −COOH group of *p*-ER chemically bonds with the Ti atoms of the TiO_2 and displaces the surrounding ACN solvent from the TiO_2 surface. Conversely, in EtOH, which binds strongly with TiO_2 to form a solvent shell around TiO_2, *p*-ER is unable to displace the EtOH solvent. Instead, *p*-ER adsorbs onto the surface of the EtOH solvation shell coating the TiO_2 particle.

We then ask the following question: Why does a smaller density of *p*-ER on TiO_2 in ACN give more SHS signal than the protic solvent cases where more *p*-ER are adsorbed on the particle? Here we recognize that in addition to adsorption density, factors like the ensemble orientation and intermolecular interactions of the molecules on the surface may strongly affect the SHS intensity.

First, consider the orientation of *p*-ER at the particle surface in different solvents. It is reasonable to assume that *p*-ER molecules are aligned in the same orientation when they adsorb directly on the TiO_2 surface with the −COOH group chemically bound to the Ti atoms.[50] In contrast, *p*-ER adsorbed on the surface of the EtOH solvation shell, where the interaction is weaker and the solvent shell molecules may not be as ordered as the TiO_2 surface atoms, may not have the same alignment and therefore yields a more disordered orientation. Consequently, the ensemble average of the molecular hyperpolarizability of the aligned molecules on the TiO_2 surface may result in a much larger surface susceptibility than that of the more disoriented molecules on the solvent shell.

Time-dependent DFT calculations were performed in order to characterize the magnitude and relative spatial orientation of the resonantly enhanced first hyperpolarizability tensor components, $\beta(-2\omega;\omega,\omega)$, of *p*-ER in both protic (EtOH) and aprotic (ACN) solvents. Specifically, we calculated the $\beta(-2\omega;\omega,\omega)$ components at 2ω = 400 nm, which is in near resonance with the predicted S_2 state of *p*-ER. The molecular frame orientation of the $\beta(-2\omega;\omega,\omega)$ components were predicted to be relatively invariant with respect to solvents, in which the main projections were aligned predominantly along the major in-plane molecular axis (*x*-axis), and (to a lesser extent) along the out-of-plane axis (*z*-axis). However, the magnitude of $\beta(-2\omega;\omega,\omega)$ showed a clear solvent dependency in which $\beta(-2\omega;\omega,\omega)$ for ACN was predicted to be ca. 25% larger than that for EtOH (i.e., 2.55 × 10^{-26} esu vs 1.91 × 10^{-26} esu). These calculations further substantiate the validity of the proposed adsorption models.

V.B. Protic Solvents Bind More Strongly than *p*-ER with TiO_2. A key factor influencing the adsorption behaviors of the carboxylic anchoring group of *p*-ER to TiO_2 under different solvent environments is that, as compared to *p*-ER, protic solvent molecules tend to bind more strongly with TiO_2. To demonstrate this point, we examine the competitive nature of absorption between *p*-ER and EtOH on TiO_2 particles.

Specifically, we examined what would happen to the measured SHS signal from a *p*-ER in TiO_2/ACN sample following addition of increasing concentrations of EtOH. If protic solvents, such as EtOH, do indeed exhibit stronger interactions with the TiO_2 surface, the expected result should be a reduction in the measured SHS signal as *p*-ER is displaced from the TiO_2 surface. As depicted in Figure 3, the maximum signal is observed only in the absence of EtOH. As EtOH is introduced to the sample, and as the concentration of EtOH increases, the measured SHS signal exhibits a substantial and monotone decrease. This result strongly indicates that EtOH displaces surface adsorbed *p*-ER from TiO_2 in ACN, and likewise that EtOH exhibits stronger binding to the TiO_2 surface. This is consistent with our proposed adsorption model that, for protic solvents, *p*-ER is shielded from direct TiO_2 adsorption due to preferential binding of the solvation shell.

It should be noted that some prior studies have reported the usage of protic/alcoholic solvents in the preparation of DSSC devices.[17,21,51] Further, it has been previously reported that carboxylic-anchoring dyes, such as *p*-ER, in gaseous conditions bind to rutile TiO_2 in several different forms (e.g., bidentate, monodentate). So how can we reconcile our current observation that *p*-ER does not bind to the surface of rutile TiO_2 in the presence of an alcoholic solvent? It is important to note that during the production process of most DSSC devices, the solvent is eventually evaporated leaving behind the dye which can then interact with the TiO_2 surface. In the current study, we examine the dye-TiO_2 binding in the presence of solvent (ethanol) which exists in the colloid with orders of magnitude higher concentration than the dye. This is a very different scenario compared to the dry dye−TiO_2 electrode. Our study shows that in the presence of alcoholic solvents, *p*-ER cannot access the TiO_2 surface due to preferential binding of the excess solvent, but adsorbs onto the solvent shell surrounding the particle. However, during the drying/evaporation process, *p*-ER can adsorb to the TiO_2 surface following the loss of nearby solvent molecules. In fact, our results are actually fully consistent with prior studies examining the dye−TiO_2 interaction in the absence of solvent.

Interestingly, it is well-known that solvent selection can significantly affect the overall efficiency of DSSC devices,[16−18,52] even though the solvents are eventually removed from the electrode. The effects of solvent selection to the overall efficiency of DSSC devices, however, until recently remained to be characterized. This and our previous study on aprotic solvents[13] directly examine the interactions between the carboxylic anchoring dyes and the TiO_2 surface in the presence of solvents, and contribute to the eventual understanding of the role of solvents in making the most efficient DSSC devices.

VI. SUMMARY

The adsorption of the carboxylic anchoring dye, *p*-ER, onto TiO_2 particles in protic (e.g., EtOH, and IPA) vs aprotic (e.g.,

DOI: 10.1021/acs.jpcc.8b08513
J. Phys. Chem. C 2019, 123, 8265−8272

ACN) solvents was studied using the surface sensitive technique SHS. IR absorption spectra indicate that portions of *p*-ER in protic solvents are hydrogen bonded. Light scattering measurements show that the particle size of TiO_2 in protic solvents is about 50% larger than in the aprotic solvent. The adsorption free energy and the maximum density of *p*-ER on TiO_2 were determined from analyses of *p*-ER adsorption isotherms recorded from the SHS experiments.

Two different models for *p*-ER adsorption on TiO_2 particles were proposed for the two different types of solvents. In the aprotic solvent (ACN), *p*-ER dye molecules adsorb directly onto the TiO_2 surface and replace the adsorbed ACN molecules. In the protic solvents, however, it is assumed that the solvent molecules bind strongly with TiO_2 and form a solvent shell. Consequently, as they are unable to displace the solvent molecules, the *p*-ER molecules adsorb onto the solvent shell, but not the TiO_2 surface. Furthermore, the equilibrium between hydrogen-bonded and free *p*-ER is included in the adsorption model in which only the non-hydrogen-bonded *p*-ER adsorbs to the surface. The adsorption models can quantitatively reproduce the observed adsorption isotherms. The free energy change for adsorption in the aprotic solvent is about two kcal/mol bigger than in the protic solvents: reflecting that binding of *p*-ER directly to TiO_2 is stronger than to the protic solvent shells. Experiments depicting the competition of adsorption between *p*-ER and ethanol on TiO_2 in ACN further illustrate that the protic solvent molecules bind stronger than *p*-ER with TiO_2.

Analyses show that there are 10 times more *p*-ER on the protic solvent shell than on the TiO_2 in aprotic solvent, even though the SHS intensity is stronger for the aprotic solvent case. This observation is consistent with the adsorption model in that *p*-ER moieties directly adsorbed on TiO_2 are aligned in the same direction and result in larger surface susceptibility. In contrast, more *p*-ER can adsorb on the solvent shell but with less alignment and thus smaller susceptibility.

These findings show that, for protic solvents, the carboxylic anchoring dye molecules (like *p*-ER) do not adsorb directly on TiO_2; instead, they adsorb on the solvent shell that is around the TiO_2 particles. On the basis of this observation, it is reasoned that aprotic solvents (ACN) are more suitable for mediating adsorption of carboxylic dyes on TiO_2 for DSSC applications.

AUTHOR INFORMATION

Corresponding Author

*(H.-L.D.) E-mail: hldai@temple.edu.

ORCID

Hui Fang: 0000-0002-4024-1234

Michael J. Wilhelm: 0000-0002-4634-9561

Yi Rao: 0000-0001-9882-1314

Hai-Lung Dai: 0000-0001-6925-8075

Present Address

§Y.R.: Department of Chemistry and Biochemistry, Utah State University

Notes

The authors declare no competing financial interest.

ACKNOWLEDGMENTS

This research was funded by the department of the Army Basic Research Program through the Edgewood Chemical and Biological Center, U.S. Army Research Office (W911NF-15-2-0052).

REFERENCES

(1) O'Regan, B.; Gratzel, M. A Low-Cost, High-Efficiency Solar-Cell Based on Dye-Sensitized Colloidal Tio2 Films. *Nature* **1991**, *353*, 737−740.

(2) Hagfeldt, A.; Boschloo, G.; Sun, L. C.; Kloo, L.; Pettersson, H. Dye-Sensitized Solar Cells. *Chem. Rev.* **2010**, *110*, 6595−6663.

(3) Song, X.; Primorac, E.; Kuhlenbeck, H.; Freund, H.-J. Decoupling a Thin Well-Ordered TiO2(110) Layer from a TiO2(110) Substrate with a Ti + Ta Mixed Oxide Interlayer. *J. Phys. Chem. C* **2016**, *120*, 8185−8190.

(4) Unterberger, W.; Lerotholi, J. T.; Kröger, A. E.; Knight, J. M.; Duncan, A. D.; Kreikemeyer-Lorenzo, D.; Hogan, A. K.; Jackson, C. D.; Włodarczyk, R.; Sierka, M.; et al. Local Hydroxyl Adsorption Geometry on TiO2(110). *Phys. Rev. B: Condens. Matter Mater. Phys.* **2011**, *84*, 115461.

(5) Chen, X.; Mao, S. S. Titanium Dioxide Nanomaterials: Synthesis, Properties, Modifications, and Applications. *Chem. Rev.* **2007**, *107*, 2891−2959.

(6) Velusamy, M.; Justin Thomas, K. R.; Lin, J. T.; Hsu, Y. C.; Ho, K. C. Organic Dyes Incorporating Low-Band-Gap Chromophores for Dye-Sensitized Solar Cells. *Org. Lett.* **2005**, *7*, 1899−1902.

(7) Linsebigler, A. L.; Lu, G. Q.; Yates, J. T. Photocatalysis on Tio2 Surfaces - Principles, Mechanisms, and Selected Results. *Chem. Rev.* **1995**, *95*, 735−758.

(8) Zhang, L.; Cole, J. M. Anchoring Groups for Dye-Sensitized Solar Cells. *ACS Appl. Mater. Interfaces* **2015**, *7*, 3427−3455.

(9) Imahori, H.; Umeyama, T.; Ito, S. Large Π-Aromatic Molecules as Potential Sensitizers for Highly Efficient Dye-Sensitized Solar Cells. *Acc. Chem. Res.* **2009**, *42*, 1809−1818.

(10) Cahen, D.; Hodes, G.; Grätzel, M.; Guillemoles, J. F.; Riess, I. Nature of Photovoltaic Action in Dye-Sensitized Solar Cells. *J. Phys. Chem. B* **2000**, *104*, 2053−2059.

(11) Koops, S. E.; O'Regan, B. C.; Barnes, P. R. F.; Durrant, J. R. Parameters Influencing the Efficiency of Electron Injection in Dye-Sensitized Solar Cells. *J. Am. Chem. Soc.* **2009**, *131*, 4808−4818.

(12) Murakoshi, K.; Kano, G.; Wada, Y.; Yanagida, S.; Miyazaki, H.; Matsumoto, M.; Murasawa, S. Importance of Binding States between Photosensitizing Molecules and the Tio2 Surface for Efficiency in a Dye-Sensitized Solar-Cell. *J. Electroanal. Chem.* **1995**, *396*, 27−34.

(13) Fang, H.; Xu, B.; Li, X.; Kuhn, D. L.; Zachary, Z.; Tian, G.; Chen, V.; Chu, R.; DeLacy, G. B.; Rao, Y.; et al. Effects of Molecular Structure and Solvent Polarity on Adsorption of Carboxylic Anchoring Dyes onto TiO2 Particles in Aprotic Solvents. *Langmuir* **2017**, *33*, 7036−7042.

(14) Gregg, B. A. Interfacial Processes in the Dye-Sensitized Solar Cell. *Coord. Chem. Rev.* **2004**, *248*, 1215−1224.

(15) Zhang, L.; Cole, J. M.; Liu, X. Tuning Solvatochromism of Azo Dyes with Intramolecular Hydrogen Bonding in Solution and on Titanium Dioxide Nanoparticles. *J. Phys. Chem. C* **2013**, *117*, 26316−26323.

(16) Lee, K.-M.; Suryanarayanan, V.; Ho, K.-C. Influences of Different Tio2Morphologies and Solvents on the Photovoltaic Performance of Dye-Sensitized Solar Cells. *J. Power Sources* **2009**, *188*, 635−641.

(17) Al-Alwani, M. A. M.; Mohamad, A. B.; Kadhum, A. A. H.; Ludin, N. A. Effect of Solvents on the Extraction of Natural Pigments and Adsorption onto TiO2 for Dye-Sensitized Solar Cell Applications. *Spectrochim. Acta, Part A* **2015**, *138*, 130−137.

(18) Ono, T.; Yamaguchi, T.; Arakawa, H. Influence of Dye Adsorption Solvent on the Performance of a Mesoporous Tio2 Dye-Sensitized Solar Cell Using Infrared Organic Dye. *J. Sol. Energy Eng.* **2010**, *132*, 021101.

(19) Parker, A. J. Protic-Dipolar Aprotic Solvent Effects on Rates of Bimolecular Reactions. *Chem. Rev.* **1969**, *69*, 1−32.

(20) Fang, H.; Wu, Y.; Kuhn, D. L.; Zander, Z.; DeLacy, B. G.; Rao, Y.; Dai, H.-L. Electron Injection from a Carboxylic Anchoring Dye to

DOI: 10.1021/acs.jpcc.8b08513
J. Phys. Chem. C 2019, 123, 8265−8272

Tio2 Nanoparticles in Aprotic Solvents. *Chem. Phys.* **2018**, *512*, 93−97.
(21) Lee, J. W.; Kim, T. Y.; Ko, H. S.; Han, S.; Lee, S. H.; Park, K. H. Influence of Polar Solvents on Photovoltaic Performance of Monascus Red Dye-Sensitized Solar Cell. *Spectrochim. Acta, Part A* **2014**, *126*, 76−80.
(22) Lun Pang, C.; Lindsay, R.; Thornton, G. Chemical Reactions on Rutile TiO_2(110). *Chem. Soc. Rev.* **2008**, *37*, 2328−2353.
(23) Xu, C.; Yang, W.; Guo, Q.; Dai, D.; Chen, M.; Yang, X. Molecular Hydrogen Formation from Photocatalysis of Methanol on TiO2(110). *J. Am. Chem. Soc.* **2013**, *135*, 10206−10209.
(24) Bates, S. P.; Gillan, M. J.; Kresse, G. Adsorption of Methanol on Tio2(110): A First-Principles Investigation. *J. Phys. Chem. B* **1998**, *102*, 2017−2026.
(25) Zhang, Z.; Bondarchuk, O.; Kay, B. D.; White, J. M.; Dohnálek, Z. Direct Visualization of 2-Butanol Adsorption and Dissociation on TiO2(110). *J. Phys. Chem. C* **2007**, *111*, 3021−3027.
(26) Tran, R. J.; Sly, K. L.; Conboy, J. C. Applications of Surface Second Harmonic Generation in Biological Sensing. *Annu. Rev. Anal. Chem.* **2017**, *10*, 387−414.
(27) Wang, H.; Troxler, T.; Yeh, A.-G.; Dai, H.-L. In Situ, Nonlinear Optical Probe of Surfactant Adsorption on the Surface of Microparticles in Colloids. *Langmuir* **2000**, *16*, 2475−2481.
(28) Wang, H.; Yan, E. C. Y.; Borguet, E.; Eisenthal, K. B. Second Harmonic Generation from the Surface of Centrosymmetric Particles in Bulk Solution. *Chem. Phys. Lett.* **1996**, *259*, 15−20.
(29) Wang, H. F.; Yan, E. C. Y.; Liu, Y.; Eisenthal, K. B. Energetics and Population of Molecules at Microscopic Liquid and Solid Surfaces. *J. Phys. Chem. B* **1998**, *102*, 4446−4450.
(30) Gonella, G.; Dai, H.-L. Second Harmonic Light Scattering from the Surface of Colloidal Objects: Theory and Applications. *Langmuir* **2014**, *30*, 2588−2599.
(31) Roke, S.; Gonella, G. Nonlinear Light Scattering and Spectroscopy of Particles and Droplets in Liquids. *Annu. Rev. Phys. Chem.* **2012**, *63*, 353−378.
(32) Haber, L. H.; Kwok, S. J.; Semeraro, M.; Eisenthal, K. B. Probing the Colloidal Gold Nanoparticle/Aqueous Interface with Second Harmonic Generation. *Chem. Phys. Lett.* **2011**, *507*, 11−14.
(33) Gan, W.; Gonella, G.; Zhang, M.; Dai, H.-L. Reactions and Adsorption at the Surface of Silver Nanoparticles Probed by Second Harmonic Generation. *J. Chem. Phys.* **2011**, *134*, 041104.
(34) Dadap, J. I.; Shan, J.; Eisenthal, K. B.; Heinz, T. F. Second-Harmonic Rayleigh Scattering from a Sphere of Centrosymmetric Material. *Phys. Rev. Lett.* **1999**, *83*, 4045.
(35) Smallwood, I. M. In *Handbook of Organic Solvent Properties*; Smallwood, I. M., Ed.; Oxford: 1996.
(36) Smith, E. R.; Maryott, A. A. Table of Dielectric Constants of Pure Liquids. *NBS CIRC 514* **1951**, 1.
(37) Yanai, T.; Tew, D. P.; Handy, N. C. A New Hybrid Exchange−Correlation Functional Using the Coulomb-Attenuating Method (Cam-B3lyp). *Chem. Phys. Lett.* **2004**, *393*, 51−57.
(38) Frisch, M. J.; Trucks, W. G.; Schlegel, B. H.; Scuseria, E. G.; Robb, A. M.; Cheeseman, R. J.; Scalmani, G.; Barone, V.; Petersson, A. G.; Nakatsuji, H.; et al. *Gaussian 09*, Revision B.01; Gaussian, Inc.: Wallingford, CT, 2009.
(39) Gan, W.; Xu, B.; Dai, H.-L. Activation of Thiols at a Silver Nanoparticle Surface. *Angew. Chem., Int. Ed.* **2011**, *50*, 6622−6625.
(40) Corn, R. M.; Higgins, D. A. Optical Second Harmonic Generation as a Probe of Surface Chemistry. *Chem. Rev.* **1994**, *94*, 107−125.
(41) Eisenthal, K. B. Liquid Interfaces Probed by Second-Harmonic and Sum-Frequency Spectroscopy. *Chem. Rev.* **1996**, *96*, 1343−1360.
(42) Feng, R.-R.; Liu, A.-A.; Liu, S.; Shi, J.; Zhang, R.; Ren, Z. In Situ Studies on the Dissociation and Photocatalytic Reactions of Ch3oh on TiO2 Thin Film by Sum Frequency Generation Vibrational Spectroscopy. *J. Phys. Chem. C* **2015**, *119*, 9798−9804.
(43) Liu, Y.; Dadap, J. I.; Zimdars, D.; Eisenthal, K. B. Study of Interfacial Charge-Transfer Complex on Tio2 Particles in Aqueous Suspension by Second-Harmonic Generation. *J. Phys. Chem. B* **1999**, *103*, 2480−2486.
(44) Liufu, S.; Xiao, H.; Li, Y. Adsorption of Poly(Acrylic Acid) onto the Surface of Titanium Dioxide and the Colloidal Stability of Aqueous Suspension. *J. Colloid Interface Sci.* **2005**, *281*, 155−163.
(45) Vittadini, A.; Selloni, A.; Rotzinger, F. P.; Grätzel, M. Formic Acid Adsorption on Dry and Hydrated TiO2 Anatase (101) Surfaces by Dft Calculations. *J. Phys. Chem. B* **2000**, *104*, 1300−1306.
(46) Zeng, J.; Eckenrode, H. M.; Dai, H.-L.; Wilhelm, M. J. Adsorption and Transport of Charged Vs. Neutral Hydrophobic Molecules at the Membrane of Murine Erythroleukemia (Mel) Cells. *Colloids Surf., B* **2015**, *127*, 122−129.
(47) Diebold, U. The Surface Science of Titanium Dioxide. *Surf. Sci. Rep.* **2003**, *48*, 53−229.
(48) Rodríguez, R.; Blesa, M. A.; Regazzoni, A. E. Surface Complexation at the TiO2(Anatase)/Aqueous Solution Interface: Chemisorption of Catechol. *J. Colloid Interface Sci.* **1996**, *177*, 122−131.
(49) Zhang, L.; Cole, J. M.; Waddell, P. G.; Low, K. S.; Liu, X. Relating Electron Donor and Carboxylic Acid Anchoring Substitution Effects in Azo Dyes to Dye-Sensitized Solar Cell Performance. *ACS Sustainable Chem. Eng.* **2013**, *1*, 1440−1452.
(50) Zhang, L.; Cole, J. M.; Dai, C. Variation in Optoelectronic Properties of Azo Dye-Sensitized TiO2 Semiconductor Interfaces with Different Adsorption Anchors: Carboxylate, Sulfonate, Hydroxyl and Pyridyl Groups. *ACS Appl. Mater. Interfaces* **2014**, *6*, 7535−7546.
(51) Ozawa, H.; Awa, M.; Ono, T.; Arakawa, H. Effects of Dye-Adsorption Solvent on the Performances of the Dye-Sensitized Solar Cells Based on Black Dye. *Chem. - Asian J.* **2012**, *7*, 156−162.
(52) Pollard, J. A.; Zhang, D.; Downing, J. A.; Knorr, F. J.; McHale, J. L. Solvent Effects on Interfacial Electron Transfer from Ru(4,4′-Dicarboxylic Acid-2,2′-Bipyridine)2(Ncs)2 to Nanoparticulate Tio2: Spectroscopy and Solar Photoconversion. *J. Phys. Chem. A* **2005**, *109*, 11443−11452.

DOI: 10.1021/acs.jpcc.8b08513
J. Phys. Chem. C 2019, 123, 8265−8272